Adsorptive Removal of Methylene Blue from Water using Magnetic Biochar from *Pentaclethra macrophylla* Seed Shells: Equilibrium, Kinetics and Thermodynamic Studies

S.C., Iromaka[1], V.O., Njoku[1], C.E. Duru[1] and O.O. John-Dewole[2]

[1]Department of Chemistry, Imo State University, Owerri, Nigeria
[2]Department of Chemical Sciences, Lead City University, Ibadan
*Correspondence: johndewole.olusegun@lcu.edu.ng ORCID 0000-0003-4883-7750
phone: +2348034968640

Abstract: The release of synthetic dyes, such as methylene blue (MB), into waterbodies poses significant environmental and health risks due to their toxicity, mutagenicity and persistence. Conventional water treatment methods often struggle to effectively remove these pollutants. However, biomass-derive adsorbent, like biochar, have potentials in removing dyes from polluted water efficiently at low cost. This study investigated the use of magnetic impregnated biochar of *Pentaclethra macrophylla* (African oil bean) seed shell (F_e-BC PM) as an adsorbent to remove MB by employing batch adsorption experimental set-up. The adsorbent was characterized by Fourier Transform Infrared (FTIR) spectroscopy, scanning electron microscopy (SEM) and Brunauer Emmett Teller (BET) for surface area and pore size analysis. Experimental adsorption data were modeled with such isotherm models as Langmuir, Freundlich, Temkin and Dubinin-Radushkevich. Langmuir Isotherm best fitted the adsorption process indicating monolayer adsorption and a monolayer adsorption capacity calculated, q_m was 29.07 mg/g. Four adsorption kinetic models were experimented (Lagergren pseudo-first-order, Ho and Mckay Pseudo-second-order, intraparticle diffusion and Elovich). Pseudo-second-order (PSO) best fitted the adsorption process, using the regression coefficient (R^2) values obtained as basis. This indicated that the rate-limiting step of the adsorption process was chemisorption. The thermodynamic parameters suggest exothermic nature, increased randomness or disordering and spontaneity of the adsorption of MB onto F_e-BC at 30 ^oC, 35 ^oC, 40 ^oC, 45 ^oC, and 50 ^oC. The experimental results showed that high pH favoured the adsorption of MB onto magnetic impregnated biochar (Fe-BC) of *Pentaclethra macrophylla* seed shell. The FTIR spectral analysis indicated the presence of – OH of carboxylic acid, C-O of alcohol and C-Cl of alkyl halide all of which were functional groups identified on the Fe-BC surface.
[S.C., Iromaka, V.O., Njoku, C.E. Duru and O.O. John-Dewole. **Adsorptive Removal of Methylene Blue from Water using Magnetic Biochar from *Pentaclethra macrophylla* Seed Shells: Equilibrium, Kinetics and Thermodynamic Studies.** *Researcher* 2025;17(11):9-23]. ISSN 1553-9865 (print); ISSN 2163-8950 (online). http://www.sciencepub.net/researcher. 02. doi:10.7537/marsrsj171125.02

Keywords: *Pentaclethra macrophylla;* magnetic biochar; methylene blue dye; adsorption isotherms; adsorption kinetics

Introduction

Water pollution is the primary cause of clean water deficiency. Growing industrialization has produced large amount of untreated wastewater in man's environment. One of the most water consuming industries is textile industry. This industry is listed as the main contributor of water pollution because of the huge amount of wastewater containing dyes it pumps into our environment[1].Estimation of (17 – 20) % of world industrial water pollution is as a result of treatment and dyeing of textiles, notably that over 7 x 10^5 tonnes of dyes are produced annually[2,3]. Hence, discharged wastewater containing dyes even in the smallest quantity can be inimical to the environmental health. Aside textile industries dyes are discharged also from dyestuff manufacturing, food, cosmetics, printing and leather manufacturing industries[4].

Methylene blue (MB) is a heterocyclic aromatic compound and is one of the most important and widely used dyes in textile and paper industries. It is a dark-green odourless solid at room temperature[5,6,7].

Dyes, including MB, when present even in small amount in water causes serious aesthetic problems, interferes with penetration of sunlight into water leading to retardation of photosynthesis, aquatic biotics growth inhibition and interference with solubility of gases in water bodies[8]. Removal of MB from effluents is necessary in order to make the waterbody clean and to protect human health and water resources from pollution hazards. Due to problems associated with wastewater containing dyes, several methods including chemical oxidation, sedimentation, coagulation, ion exchange, solvent extraction, chemical precipitation, filtration,

electrolysis have been developed[9,10,11]. These methods have their disadvantages and limitations[9,12].

The advantages that adsorption process of removal have over the conventional methods of wastewater treatment include; high selectivity, low cost, efficient energy and non-denaturing. Activated carbon is very expensive in its use adsorptive pollution control because commercial carbon is very costly. Recent studies on adsorptive removal of pollutants use cheaper and renewable materials as agricultural wastes and by products as adsorbents[13,14].

These recyclable phtyo-based adsorbent include; banana stalk, cocoa pod husk, cocoa pod husk, groundnut hull, oil palm fibre, cassava peels, maize husk, maize husk lignocellulose [15,16,17]. Biomass of all these agricultural wastes is usually converted to biochar for more effective and efficient adsorbent materials [18]. Biochar is a carbon-rich solid obtained from heating biomass with little or no oxygen[19]. Properties of biochar such as large specific surface area, porous structure, enriched surface functional groups make it suitable for use as good adsorbent for the removal of pollutants from aqueous solutions. Biochar porous structure is similar to that of activated carbon[20].

African Oil Bean Tree (*Pentaclethra macrophylla)* is the sole member of the genus occurring naturally in the humid lowlands of West Africa. *Pentaclethra macrophylla* (PM) has been cultivated in Nigeria since 1937 and for many years in other West African countries where its seed is relished as food[21]. PM is a major component of the agroforest system. Its seed is used as food, edible oil and in craft as bead. The seed shell has no known use for now[21,22]. After making use of the useful parts, the seed shells are littered about the environment constituting menace. The shells are difficult to biodegrade. This work produced biochar of the PM, prepare magnetite (Fe_3O_4) using Fe^{2+} and Fe^{3+} and impregnate the magnetite on the biochar, then use the magnetic impregnated composite (F_e-BC) to remove methylene blue dye from aqueous solution.

Materials and Methods

Preparation of Methylene Blue Solution

The MB solution used as an adsorbate in this work was prepared by dissolving 1.0 g of MB powder in 1,000 cm^3 of solution using, distilled water to obtain the stock solution of 1,000 mg/L. Working solutions of 25 to 250 mg/L were prepared from the stock by serial dilution using equation 1 below:

$C_1V_1 = C_2V_2$ ---------- 1

Where C_1 and C_2 are the stock and working solution concentrations respectively V_1 and V_2 are volume of stock and working solutions respectively.

Preparation of the Adsorbent

PM seeds were obtained from the tree in Obowo, Imo State, Nigeria, shelled and the seed shells washed four times with tap water. It was further washed three times with distilled and deionized water, sun-dried for four days and ground into small particle size using manual grinder (Corona, Landers YC1A. S.A. Table top, S.A). It was further ground using electric grinder (Corona mills, REF 121, S.A.) and oven-dried at 105 ^{0}C for 8 hr to constant weight using the laboratory oven (LG, MC 2886, China). The ground, dried seed shells were sieved with required mesh size (600 μm and 841 μm). The prepared sample was then pyrolysed in the electric furnace (Drawell XRF Scientific, SX3-3-12, Mainland, China) at 600 ^{0}C for 2 hr at heating rate of 10 ^{0}C/min. Nitrogen gas at flow rate of 0.1 m^3/hr was used as purge gas to keep the whole process inert[23]. The biochar produced was cooled to 30 ^{0}C and stored in air tight container after milling into powder and sieving with laboratory mesh size of 30 and 20 (600μm and 841μm).

The sample was later modified by magnetic impregnation of the biochar. Magnetite (Fe_3O_4) was synthesized according to the method of alkaline co-precipitation of iron salts ($F_eCl_2.4H_2O$ and $F_eCl_3.6H_2O$)[24].

Aqueous solutions of the iron salts were mixed in alkaline medium in the proportion of F_e^{2+} F_e^{3+} = 1:2. Initially 2MHCl solution was added to prevent oxidation of F_e^{2+} and precipitation of F_e^{3+} in the form of hydroxide. Equal volumes of molar solutions of the F_e^{3+} and F_e^{2+} in molar ratio of 2:1 were mixed and agitated for three minutes. 25 % of NH_4OH was now added into the binary solution of F_e salts under constant stirring for 30 min at room temperature. NH_4OH precipitated the nanoparticles (the black precipitate of (Fe_3O_4) which was then collected by magnet and washed with distilled water several times till the pH of the resulting wash off solution reached 9. The nanoparticles were dried at 40 ^{0}C for 24 hr. Equation 2 below describes the process.

$$F_e^{2+}(aq) + 2\ F_e^{3+}(aq) + 8\ OH^-(aq) \longrightarrow Fe_3O_4 + 4\ H_2O \quad \ldots\ldots\ldots 2$$

NH_4OH must be added into the binary (F_e^{2t}+F_e^{3t}) solution and not the other way round.

Iron/Biochar composite was then prepared by impregnation mass ratio of Biochar (BC) powder: Fe_3O_4 (aq) = 1:1 and then pyrolysed at 1000^{0}C in a N_2 – purged tubular furnace. The final product is the magnetic impregnated biochar (F_e-BC) of the PM[25].

Characterization of the Fe-BC Adsorbent

Textural characterization of the adsorbent was done using Quantachrome high speed surface area and pore size analyzer model: Nova 4200, USA. Brunauer – Emmette – Teller (BET) surface area, Berrett-Joyner-Halenda (BJH) pore size and pore volume determination of the F_e-BC were then made. Agilent

Technologies Microlab Cary 630 Fourier Transform Infrared (FTIR) spectrophotometer was employed to record the spectra of the Fe-BC adsorbent in the investigation of the surface chemistry of the adsorbent. Data analysis was focused on the 400 to 4000cm^{-1} region. The sample was formed into pellets with potassium bromide (KBr). 1mg of Fe-BC was encapsulated in 100 mg of KBr for the infrared (IR) study. The adsorbent (before and after adsorption) were collected in transmission and the background correct in each case. The shift in the adsorption band of the FTIR spectra in the adsorbent after adsorption from those of the adsorbent before adsorption gave an insight on the functional groups responsible for the adsorption of MB. Scanning Electron Microscope (SEM), Phenom Prox model, Phenom World Einfhoven, The Netherlands was used to examine the morphology and structure of the Fe-BC adsorbent before and after MB adsorption. Point of zero charge (pHpzc), the pH at which the surface of an adsorbent is neutral was determined using pH drift method[25]. The pHpzc was determined by adding 0.1g of the adsorbent sample (Fe-BC) to 95 cm^3 of 0.01 m NaCl solution in each of eleven 250 cm^3 conical flasks. The pH values were adjusted using dilute HCl and NaOH as the case was required[25].

Batch Adsorption Study

The batch adsorption experiments were conducted using 200 cm^3 of the prepared working solutions as initial dye solution concentrations. 1 g of the adsorbent, Fe-BC, was agitated at 120 rpm in each 250 cm^3 flask containing initial dye concentration (25, 50, 100, 150, 200 or 250 mg/L MB). The effect of the initial solution pH on the adsorption of MB in aqueous solution using Fe-BC was carried out by contacting 200 cm^3 of 150 mg/L MB solution with 1g magnetic impregnated biochar of the African oil bean seed shell (Fe-BC) in different flasks containing the MB dye solution adjusted to pH values 2 to 12 respectively. The mixture was agitated for 170 min at 30 ^{0}C in water bath shaker and supernatant liquid withdrawn, filtered and the absorbance determined using UV- Visible spectrophotometer (Shimadzu UV-752, M/s. Shimadzu, Japan) at wavelength of 663 nm (wavelength of maximum absorbance of methylene blue dye).

The amount of MB adsorbed per unit mass of adsorbent at equilibrium, q_e (mg/g) was found using equation (3).

$$q_e = \frac{(C_o - C_e)\,V}{m} \text{ ---------- (3)}$$

Where C_o = initial MB concentration in liquid phase;
C_e = liquid phase MB concentration at equilibrium. The units of C_o and C_e are mg/L.
V = Volume of MB solution (L)
m = mass of dry adsorbent used (g)

Removal percent, R % was calculated using Equation (4)

$$R\,\% = \frac{C_o - C_e}{C_o} \times \frac{100}{1} \text{ ----------} \quad (4)$$

Where C_o and C_e are as in equation (3)

The effect of initial dye concentration and contact time on the adsorption of MB by Fe-BC was determined by varying the contact time (10 to 200 min) for 200 cm^3 of each initial dye concentration (25 - 250 mg/L) at constant temperature of 30 ^{0}C. Each initial dye concentration and adsorbent dose mixture was agitated for different studied time and at the end of each studied time, small amount of the solution was taken out of the water bath shaker and the supernatant liquid filtered with 0.45 μm membrane filter after diluting 1 cm^3 to 20 cm^3 using distilled water as in other effects investigation. The absorbance of the resulting solution was determined using UV- Visible spectrophotometer. q_t and R% were obtained using equation (5) and (6)

$$q_t = \frac{(C_o - C_t)V}{m} \text{ ---------- (5)}$$

$$R\,\% = \frac{C_o - C_e}{C_o} \times \frac{100}{1} \text{ ----------} \quad (6)$$

Where q_t is amount of MB adsorbed per unit mass of adsorbent at time, t. Unit of q_t is mg/g.

C_t is liquid phase MB concentration at time, t. Unit of C_t is mg/L. Co, V and m are as described in equation (3)

The effect of Temperature on the adsorption of MB dye was carried out by varying the temperature (30 to 50 %) at constant initial concentration (150 mg/L), constant adsorbent mass (1 g) and constant pH (10). 200 cm^3 of 150 mg/L MB was taken into a conical flask containing 1 g of the adsorbent and agitated in a water bath at the required temperature and at a fixed agitation speed of 120 rpm over a given time (120 min). The absorbance of the solution at each temperature of determination was read after filtration as in the effects of initial concentration and contact time and effect of pH.

q_e and R % at each investigated temperature were obtained using equations (3) and (4) respectively.

Triplicate measurements were made and the mean used in this investigation.

RESULTS AND DISCUSSION

Characterization of the Magnetic impregnated biochar (Fe-BC) of the *Pentaclethra macrophylla* (PM)

The FTIR results before and after adsorption onto Fe-BC is shown in table 1 and the FTIR spectra on figure 2.

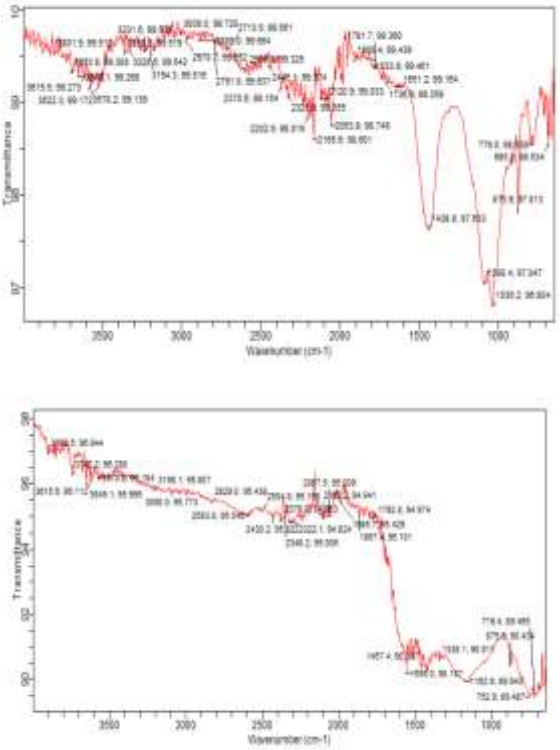

(a)

(b)

Figure 2: FTIR Spectra of Fe-BC (a) before (b) after adsorption.

The FTIR analysis identified the functional groups present in the adsorbent that are responsible for adsorption of the MB molecules. The strong intense broadband at 3194 cm^{-1} and 2791 cm^{-1} can be ascribed to the –OH vibration of the carboxylic acid group of the Fe-BC. These bands were shifted respectively to 3198cm^{-1} and 2828cm^{-1} and were therefore involved in adsorption of MB molecules. The peaks at 3328cm^{-1} and 2120cm^{-1} may be due to C-H stretching vibration of alkyne group of the adsorbent. Both of them disappeared from the spectra after adsorption indicating that both were used for adsorption. Peaks at 1088cm^{-1} and 1036cm^{-1} are medium intensed C-O stretching vibration ascribed to carbonyl group which were used for adsorption as they did not show up in the spectra of the FTIR obtained after adsorption. The other prominent peak at 779cm^{-1} is a strong intense C-Cl stretching vibration ascribed to alkyl halide functional group. It was shifted to 752cm^{-1} in the spectra after adsorption. Also the peak at 1651cm^{-1} is C=C stretching vibration denoting alkene functional group. The peak was not there after using the sample for adsorption. It was used for adsorption.

The Scanning Electron Microscopy (SEM) images of the Fe-BC (a) before and (b) after adsorption were shown in figure 2a and 2b. Figure 2a showed a large number of pores which were drastically reduced after adsorption (figure 2b). This indicated that adsorption have taken place sufficiently. The pore distribution and surface of the adsorbent were irregular. The size and number of pores indicated the expected adsorption result of MB onto Fe-BC.

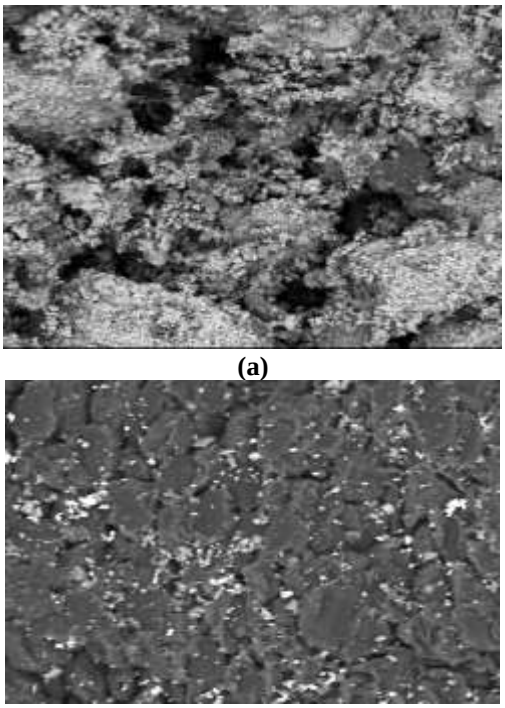

(a)

(b)

Figure 3: SEM images of Fe-BC (a) before adsorption (b) after adsorption of MB dye.

BET and BJH analysis of the Fe-BC adsorbent were carried out and the results of the surface area, pore volume and pore diameter of Fe-BC are shown in table 2.

Table 2: BET and BJH result of Fe-BC

Characterization of Adsorbent	Values Obtained
Surface area (m^2/g)	411.000
Pore volume (CC/g)	0.127
Pore diameter (nm)	2.100

The Fe-BC, from values in table 2, is a mesoporous material (with 2.100 nm pore diameter). Hence Fe-BC is a potential adsorbent justified by the result of the adsorption of this work. pHpzc analysis on Fe-BC showed that the point of zero charge lies at about pH 6.7. This gives indication that adsorption of MB using Fe-BC might record reasonably high q_e values from pH 6.7 and above. The graph of ΔpH (pH_f-pH_i) against pH_i is displayed in figure 4.

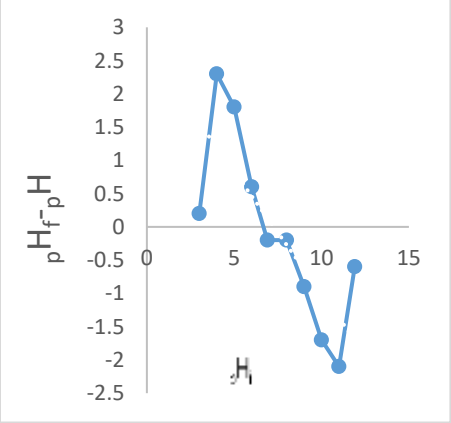

Figure 4: Graph for pHpzc of Fe-BC

Effect of Initial Dye Concentration and Contact Time

The influence of initial dye concentration and contact time in equilibrium uptake of MB onto Fe-BC is depicted in figure 5.

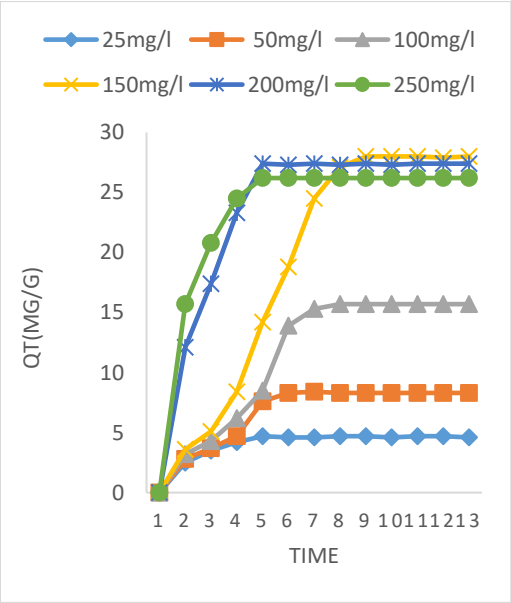

(a)

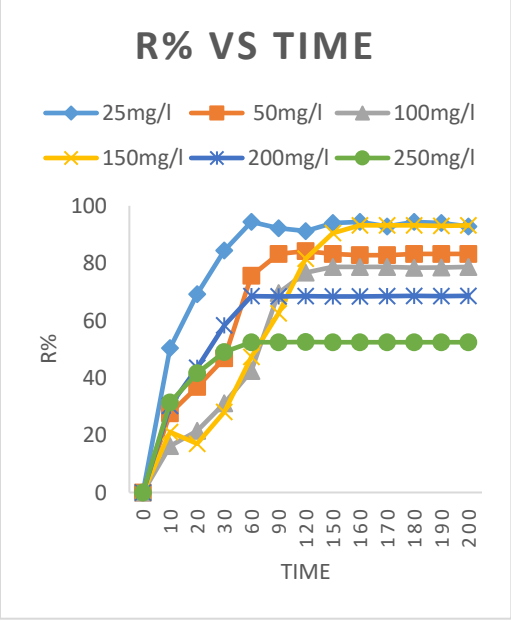

(b)

Figure 5: Initial Dye Concentration and Contact Time on the Adsorption of MB by Fe-BC (a) Adsorption Capacity, and (b) Percent Removal (R %)

As depicted in figure 5a, adsorption capacity (q_t) increased with increase in initial MB concentration. This trend is due to increasing concentration gradient acting as increasing driving force to overcome all mass transfer resistances of the MB molecules between the aqueous and solid phase. This lead to increasing equilibrium adsorption capacity, q_t until adsorbent surface sites saturation was attained[26,27]. The percent removal, R % decreased with increase in initial

dye concentration as shown in figure 5b. The removal percent, R % of the adsorption of MB by Fe-BC recorded highest value of 94.4 % at a contact time of 180 mins for initial dye concentration of 25 mg/L. This result is relative to previous adsorption reports[28,29]. Most MB molecules present in the solution were able to interact with binding sites on the surface of the adsorbent at low concentrations. This lead to higher yield in the adsorption (R %) as observed at 94.4 %. Since, all adsorbents have limited number of binding sites, creating binding saturation at a certain concentrations[28]. This might be responsible for more of the MB molecules that were left unadsorbed at higher concentrations.

Effect of Solution pH

Solution pH is one of the most important parameters affecting adsorption process. It affects the surface charge of adsorbents, the degree of ionization and speciation of adsorbate[30]. The ability of hydrogen ions to compete with ions of adsorbate on active sites of the adsorbent surface is directly related to the effect of initial solution pH. The effect of initial solution pH on the adsorption of MB onto Fe-BC is depicted in figures 6.

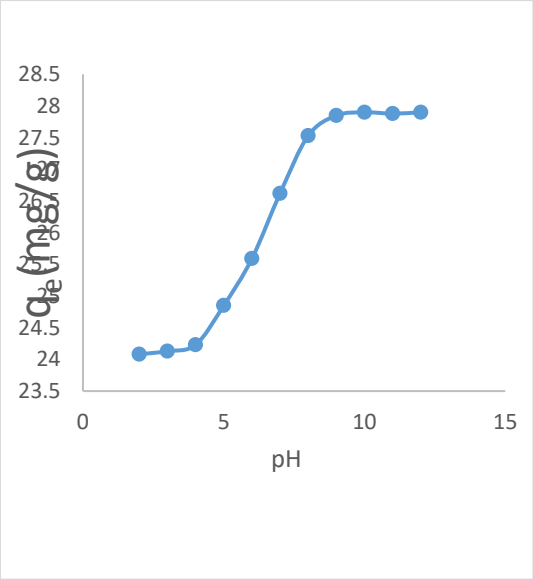

(a)

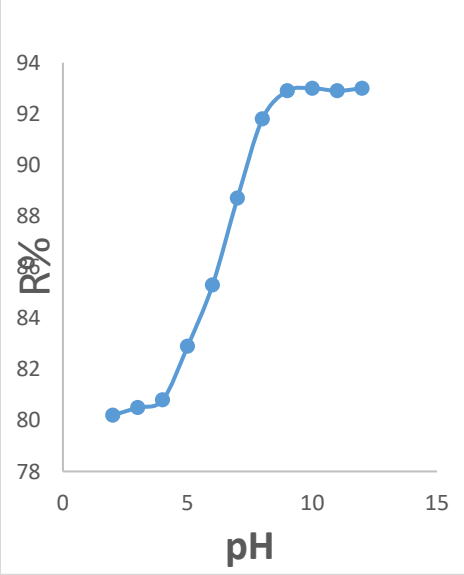

(b)

Figure 6: Effect of initial solution pH on the adsorption of MB onto Fe-BC (a) q_e (b) R%

Adsorption potential of Fe-BC for MB dye increased with increase in solution pH slowly from pH 2 to pH 4 and increased rapidly after pH 5 till pH 9. It then slowed down again from pH 10 to pH 12. From the pHpzc determined for Fe-BC, the point of zero charge pH of Fe-BC was at about pH 6.7. It was observed from figure 5 that the sharp rise in q_e occurred close to the pHpzc value. At the lower pH values, H^+ ions were competing with the cation groups of MB for sites of adsorption. The H^+ surface charge density decreased with increase in solution pH. The electrostatic repulsion between the MB dye (which is positive) and the adsorbent surface reduced. This might have resulted in increase in adsorption rate [31].

Effect of Temperature

The range of temperatures investigated in this study were 30, 35, 40, 45 and 50^{0}C. The result is depicted in figure 7.

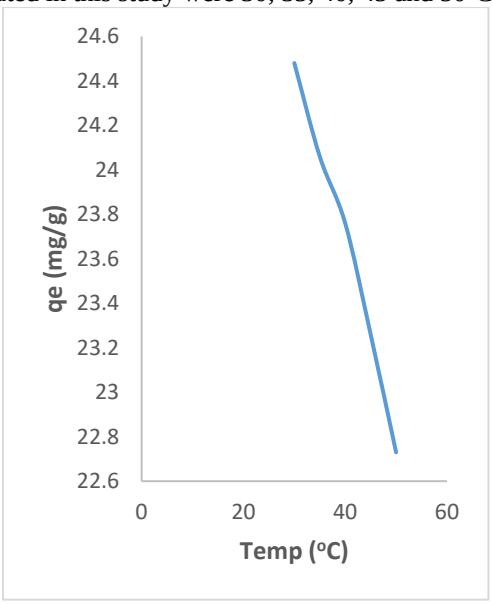

(a)

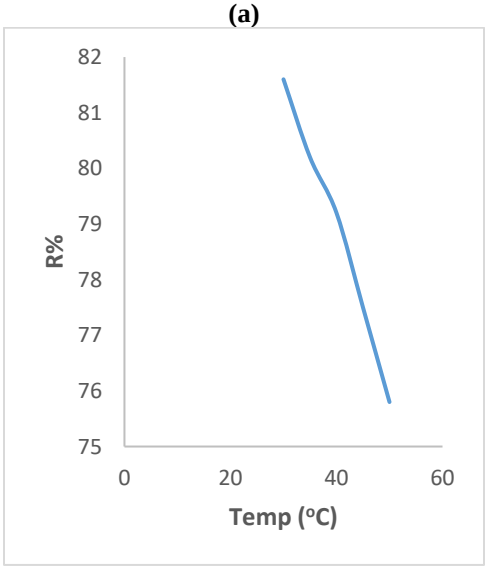

(b)

Figure 7: Effect of temperature on the adsorption of MB onto Fe-BC (a) Adsorption capacity (b) Removal percent

Increase in temperature resulted in decrease in the adsorption capacity (q_e) as seen in figure 7. The highest q_e value of 24.48 mg/g was recorded at 30 ^{0}C. The decrease in q_e with increase in temperature can be attributed to desorption[32].

The desorption may be caused by increase in available thermal energy. Decrease in adsorption with increase in temperature indicated weak adsorption interaction between adsorbent and adsorbate[33].

Adsorption Kinetics

The Lagergren pseudo-first-order, Ho and Mckay pseudo-second-order, intra-particle diffusion and Elovich models were used to determine the rate constants of the adsorption processes.

Results of the kinetic models are displayed on figures 8, 9, 10 and 11 for Pseudo-first order (PFO), Pseudo-second-order (PSO), intra-particle diffusion (ID) and Elovich models respectively.

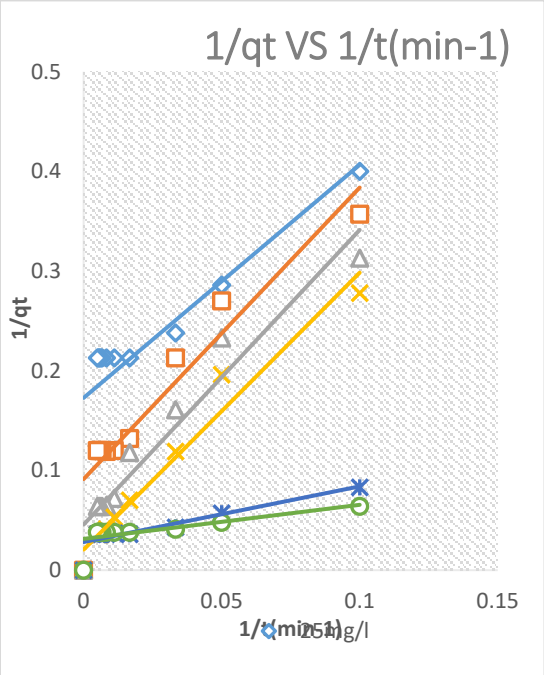

Figure 8: Pseudo First Order (PFO) Kinetic Model for Fe-BC

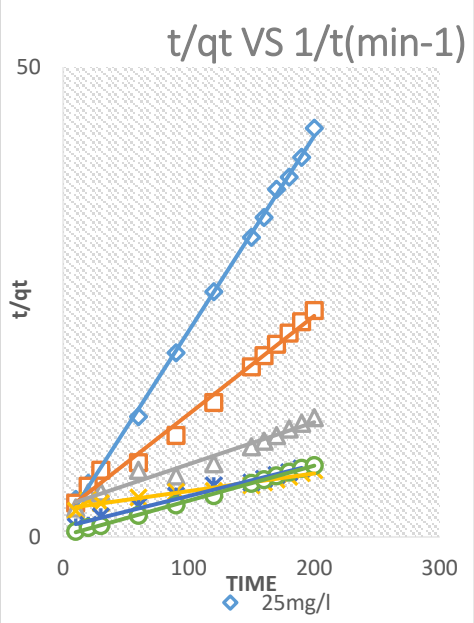

Figure 9: Pseudo Second Order (PSO) Kinetic Model for Fe-BC

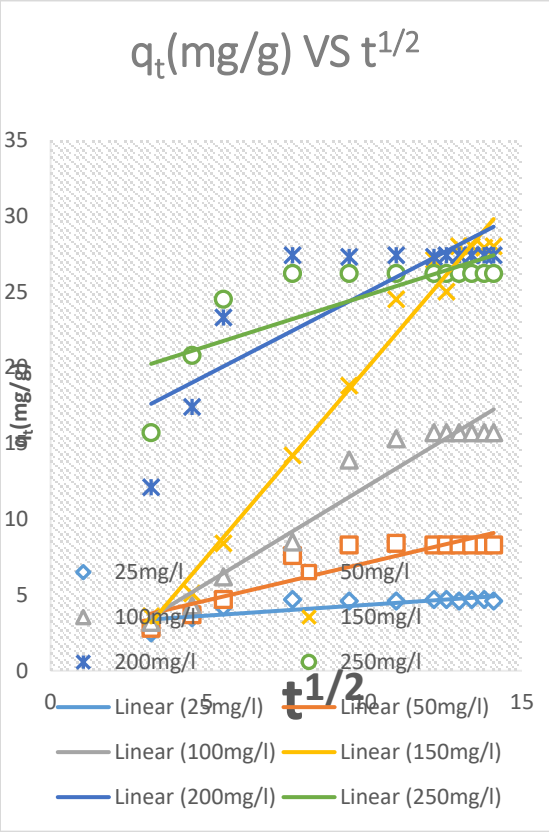

Figure 10: Intraparticle Diffusion Order Kinetic Model for Fe-BC

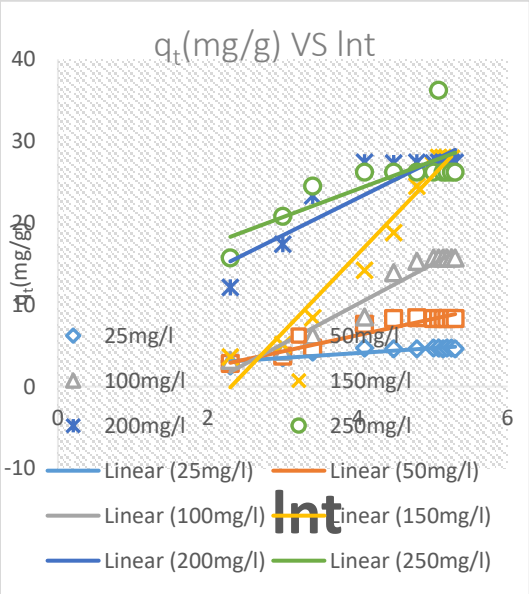

Figure 11: Elovich Kinetic Model for Fe-BC

The best fit on the kinetic models is PSO with the highest linear regression correlation co-efficient (R^2) values of approximately 0.99 at all initial dye concentrations studied. This was followed by Elovich model with R^2 (0.9619, 0.9526, 0.9168, 0.8298, 0.7931 and 0.5522) at initial dye concentrations 25, 50, 100, 150, 250 mg/L respectively. The best fit on Pseudo-second-order implies that the MB uptake rate is proportional to the number of active sites occupied

by the adsorbed dye on the adsorbent surface. It also implied that the rate controlling step was chemisorptions, according to related reports[27,28,31,32].

3.6 Adsorption Isotherms

Result of the various isotherm models are displayed in figures 12, 13, 14 and 15 below:

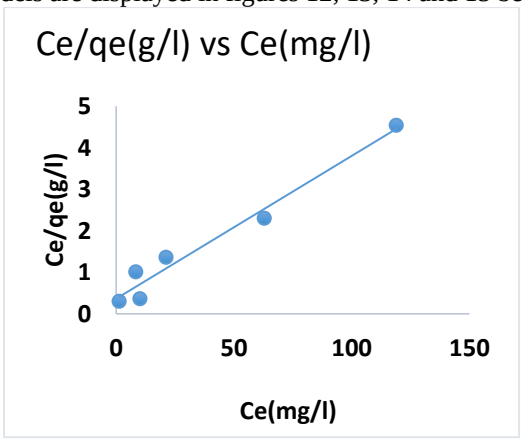

Figure 12: Langmuir Isotherm for Fe-BC of PM

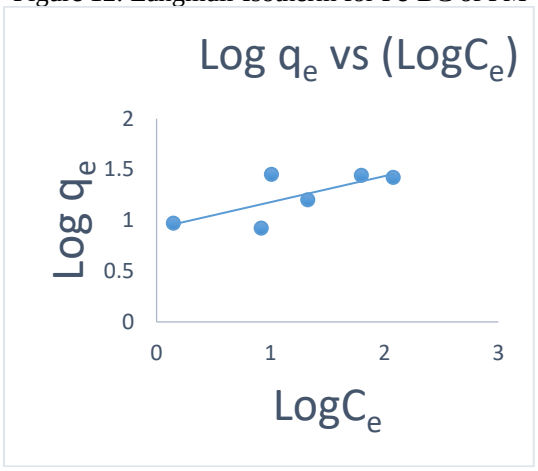

Figure 13: Freundlich Isotherm for Fe-BC of PM.

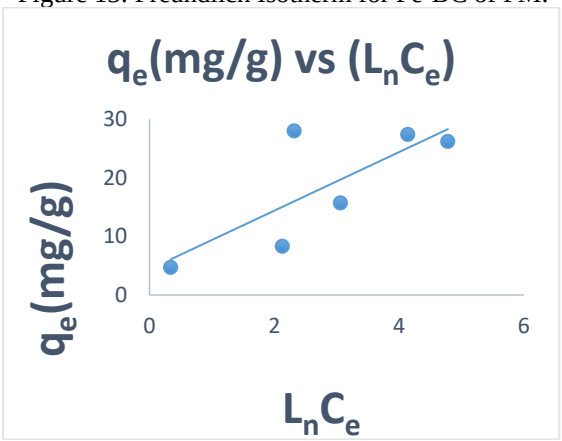

Figure 14: Temkin Isotherm Fe-BC of PM

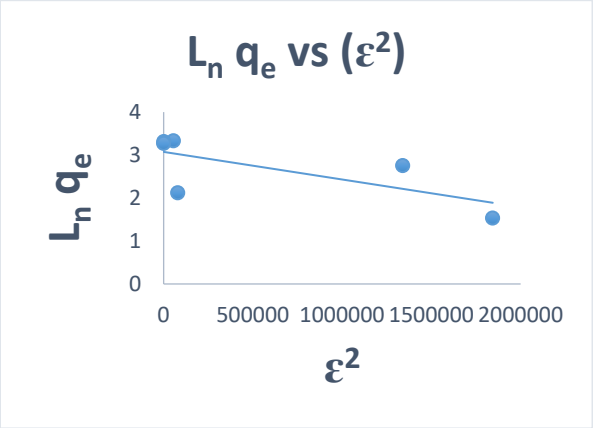

Figure 15: D-R Isotherm for Fe-BC of PM

Langmuir model recorded the highest R^2 value of 0.9690. Langmuir therefore showed the best fit for the adsorption of MB dye by Fe-BC. This implies monolayer adsorption on the surface of Fe-BC [34]. The monolayer maximum adsorption capacity (qm) calculated with the Langmuir model was 29.07 mg/g. Value of R_L obtained from Langmuir isotherm using Fe-BC is 0.0661. The R_L value of 0.0661 obtained is $0 < R_L < 1$ (that is the obtained R_L is between 0 and 1). Hence, adsorption in this case was favourable[34,35,36]. The separation factor, R_L is dimensionless.

3.7 Adsorption Thermodynamics

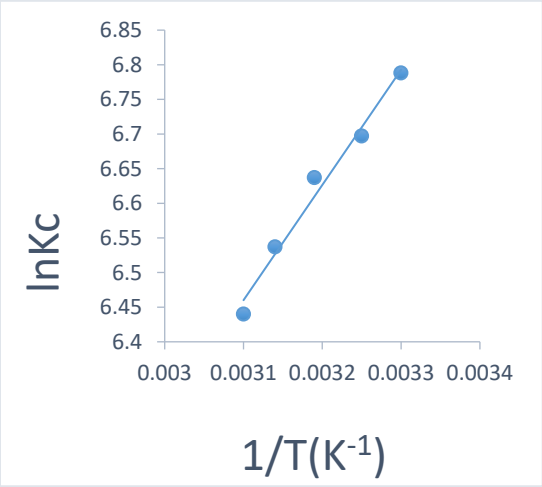

Figure 16: Van't Hoff plot for Fe-BC

In the thermodynamic study, the enthalpy change, ΔH^o as calculated is -13.832 kJ/mol showing exothermic nature of the adsorption of MB onto Fe-BC.
The entropy change, ΔS^o was +10.833 J/mole showing that the process had increasing randomness at the solid/solution interface.
At the prevailing temperatures, the values of ΔG^o were found to be negative suggesting spontaneous adsorption of MB onto Fe-BC at the temperatures used[37]. The above observations on the thermodynamic characteristics of MB adsorption onto magnetic impregnated biochar of *Pentaclethra macrophylla* can be compared with other investigations [38,39,40,41].

Conclusion

The FTIR characterization of Fe-BC showed functional groups of carboxylic, C-O, alcohol, alkyl halide, alkyne and alkene functional groups. The adsorbent was also characterized by SEM which revealed large number of pores. Surface area (m^2/g), pore volume (cc/g) and pore diameter of the adsorbent were obtained from BET and BJH analysis. From values obtained, Fe-BC is a mesoporous material. Above characteristic of Fe-BC confirm that the adsorbent has appropriate physical and chemical properties for adsorption process. The adsorption kinetics revealed high equilibrium adsorption capacity. A maximum adsorption of 29.07 mg/g was obtained from the Langmuir monolayer adsorption capacity, Langmuir model been the model where experimented data was most fitted using the isotherm models. The R_L value obtained from Langmuir model showed that the adsorption process was favourable. Pseudo-second-order model best fitted the Kinetic model suggesting that the rate controlling step was chemisorption. It also implied that the MB uptake rate was proportional to the number of active sites occupied by the adsorbed dye on the adsorbent surface. The adsorption of MB onto Fe-BC was exothermic, of increasing randomness and spontaneous at the temperatures investigated. On the overall, Fe-BC showed potential as a viable adsorbent for the removal of MB from aqueous solution.

Declaration of Competing Interest:

The authors declare that they have no conflict(s) of interest. All authors have read, understood, and have complied as applicable with the statement on "Ethical Responsibilities of Authors" as found in the Instructions for Authors in this journal.

Correspondence to:
Olusegun Onimisi, John-Dewole
Department of Chemical Sciences
Lead City University, Ibadan
Email: johndewole.olusegun@lcu.edu.ng
ORCiD 0000-0003-4883-7750

REFERENCES

1. Boddu, S., Chavali, M., Dulla, J.B., Allugunulla, V.N., Mikkili, I., Malladi, S., Mannepalli, S. and Khan, A.A., 2025. Innovative magnetic biochar for textile wastewater treatment: a sustainable solution for methylene blue and Congo Red dye removal. *Biomass Conversion and Biorefinery*, *15*(10), pp.15399-15415.
2. Wang, J., Tan, Y., Yang, H., Zhan, L., Sun, G. and Luo, L., 2023. On the adsorption characteristics and mechanism of methylene blue by ball mill modified biochar. *Scientific Reports*, *13*(1), p.21174.
3. Nnadozie, E.C. and Ajibade, P.A. (2020): Adsorption, kinetic and mechanistic studies of Pb(II) and Cr(VI) ions using APTES functionalized magnetic biochar. *Microporous Mesoporous Mater*., 309:110-573.
4. Olugbenga, S.B., Temitope, C.A., Oluwakemi, C.A. and Abimbola, M.O. (2020): Sequestering a nonsteroidal anti-inflammatory drug using modified orange peels. *Applied Water Science*, 10:172.
5. Senem, Y. and Merilyn, A. (2024): Agricultural low-cost waste adsorption of methylene blue and modeling linear isotherm method versus nonlinear prediction. *Clean Techn. Environ. Policy (Springen)*. Doi.org/10.1007/10098-02928-6.
6. Bayram, O., Özkan, U., Göde, F., Coşkun, S. and Şahin, H.T., 2025. Removal of methyl blue from aqueous solutions with nano-magnetic Pinus brutia biochar. *Journal of Dispersion Science and Technology*, *46*(11), pp.1737-1746.
7. Samaraweera, H., Rivera, A., Carter, K., Felder, T., Nawalage, S., Chui, I., Perez, F., Khan, A.H. and Mlsna, T., 2023. Green iron oxide-modified biochar for methylene blue removal from aqueous solutions. *Groundwater for Sustainable Development*, *21*, p.100945.
8. Vinayagam, R., Murugesan, G., Goveas, L.C., Varadavenkatesan, T. and Selvaraj, R., 2025. Mesoporous magnetic biochar composite through one-pot hydrothermal process for efficient degradation of methylene blue dye by Fenton-like catalysis. *Materials Technology*, *40*(1), p.2510481.
9. Chakinala, N. and Gogate, P.R., 2024. Ultrasound assisted removal of methylene blue using functionalized mesoporous biochar composites. *Chemical Engineering and Processing-Process Intensification*, *196*, p.109684.

10. Liu, Y., Wang, Z., Ma, J., Zhang, X., Feng, B., Sun, Y., Zhao, Y. and Weng, L., 2025. Sustainable removal of methylene blue and arsenic co-pollutants from wastewater using a novel Ferrihydrite@ mushroom substrate biochar composite. *Journal of Water Process Engineering*, *79*, p.108905.
11. Chistie, S.M., Naik, S.U., Rajendra, P., Apeksha, Mishra, R.K., Albasher, G., Chinnam, S., Jeppu, G.P., Arif, Z. and Hameed, J., 2025. Production and characterization of magnetic Biochar derived from pyrolysis of waste areca nut husk for removal of methylene blue dye from wastewater. *Scientific Reports*, *15*(1), p.23209.
12. Peighambardoust, S.J., Azari, M.M., Pakdel, P.M., Mohammadi, R. and Foroutan, R., 2025. Carboxymethyl cellulose grafted poly (acrylamide)/magnetic biochar as a novel nanocomposite hydrogel for efficient elimination of methylene blue. *Biomass Conversion and Biorefinery*, *15*(10), pp.15193-15209.
13. Fan, W. and Zhang, X., 2025. Magnetic coconut shell biochar/sodium alginate composite aerogel beads for efficient removal of methylene blue from wastewater: Synthesis, characterization, and mechanism. *International Journal of Biological Macromolecules*, *284*, p.137945.
14. Kataya, G., Issa, M., Badran, A., Cornu, D., Bechelany, M., Jellali, S., Jeguirim, M. and Hijazi, A., 2025. Dynamic removal of methylene blue and methyl orange from water using biochar derived from kitchen waste. *Scientific Reports*, *15*(1), p.29907.
15. Küçük, İ. and Yıldız Küçük, N., 2025. Composite Formation of Active Biochar from Pomegranate Peel with Magnetite and Alginat Beads for Methylene Blue Adsorption Using Box–Behnken Design. *Applied Sciences*, *15*(4), p.2085.
16. Zhang, Y., Li, Z., Zheng, X., Wu, Y., Wang, L. and Xie, L., 2025. Study on the adsorption of methylene blue solution by activated clay biochar composites. *Chemical Engineering Communications*, pp.1-13.
17. John-Dewole, O.O., Bamidele, M.O., Lawal I.M. and Ogundiran, A.O. Decolourisation of Methylene Blue Dye from its Aqueous Solution Using Powdered Banana Pith as Adsorbent. Nat Sci 2021;19(8):52-57.
18. Adeoye, J.B., Lau, S.Y., Tan, Y.H., Tan, Y.Y., Chiong, T., Mubarak, N.M., Anbuchezhiyan, G., Khalid, M. and Ng, J.T.W., 2025. A comprehensive review on adsorption technologies for methylene blue elimination: efficiency, mechanisms, and future perspectives. *Discover Applied Sciences*, *7*(11), p.1285.
19. Kader, N. and Değermenci, G.D., 2025. Magnetic Biochar Production from Agricultural Waste and Reactive Blue 19 Removal by Peroxymonosulfate Activation. *Fibers and Polymers*, *26*(3), pp.1197-1208.
20. Li, C., Zhang, C., Zhong, S., Duan, J., Li, M. and Shi, Y., 2023. The removal of pollutants from wastewater using magnetic biochar: a scientometric and visualization analysis. *Molecules*, *28*(15), p.5840.
21. Alazba, A.A., Shafiq, M. and Amin, M.T., 2025. Transforming Conocarpus Hedge Waste into a Highly Effective Iron/Manganese Nanocomposite Biochar for Efficient Methylene Blue Dye Removal from Aqueous Solution. *Polish Journal of Environmental Studies*, *34*(3), pp.3033-3045.
22. Nwabueze, B.I., Chiagoziem, W.C., Eboh-Ajoku, I. O., Isiuku, B.O. Njoku V.O., John-Dewole, O.O. and Akinkuotu, T.I. NaOH-Modified Plantain Stalk (nMPS) Biomass as Adsorbent for Methylene Blue from Aqueous Solution. N Y Sci J 2025;18(1):15-25.
23. Vafakish, B., Babaei-Ghazvini, A. and Acharya, B., 2025. Unraveling the mechanisms of methylene blue adsorption onto biochar: a robust and sustainable approach for water remediation. *International Journal of Environmental Science and Technology*, *22*(8), pp.7053-7064.
24. Peighambardoust, S.J., Rezaei-Aghdam, S., Niroumand, J.S., Pakdel, P.M. and Sillanpää, M., 2025. Efficient methylene blue elimination from water media by nanocomposite adsorbent-based carboxymethyl cellulose-grafted poly (acrylamide)/magnetic biochar decorated with ZIF-67. *RSC advances*, *15*(39), pp.32407-32423.
25. Guel-Nájar, N.A., Rios-Hurtado, J.C., Muzquiz-Ramos, E.M., Dávila-Pulido, G.I., Gonzalez-Ibarra, A.A. and Pat-Espadas, A.M., 2023. Magnetic biochar obtained by chemical coprecipitation and pyrolysis of corn cob residues: characterization and methylene blue adsorption. *Materials*, *16*(8), p.3127.
26. Ma, X., Li, Y., Du, Y., Chen, S., Bai, Y., Li, L., Qi, C., Wu, P. and Zhang, S., 2024. In-situ synthesis of ZIF-8 on magnetic pineapple leaf biochar as an efficient and reusable adsorbent for methylene blue removal from wastewater. *Environmental Science and Pollution Research*, *31*(16), pp.24113-24128.
27. Oyekanmi, A.A., Katibi, K.K., Omar, R.C., Ahmad, A., Elbidi, M., Alshammari, M.B. and Shitu, I.G., 2024. A novel oil palm frond magnetic biochar for the efficient adsorption of crystal violet and sunset yellow dyes from aqueous solution: synthesis, kinetics, isotherm, mechanism and reusability studies. *Applied Water Science*, *14*(2), p.13.
28. Kumar, A., Kapoor, A., Rathoure, A.K., Devnani, G.L. and Pal, D.B., 2025. Organic Compounds Removal Using Magnetic Biochar from Textile Industries Based Wastewater-A Comprehensive Review. *Sustainable Processes Connect*, *1*(1), pp.1-10.

29. Peighambardoust, S.J., Fakhiminajafi, B., Pakdel, P.M. and Azimi, H., 2025. Simultaneous elimination of cationic dyes from water media by carboxymethyl cellulose-graft-poly (acrylamide)/magnetic biochar nanocomposite hydrogel adsorbent. *Environmental Research*, *273*, p.121150.
30. Nwabueze, B.I., Nwabueze, O.O., Isiuku, B.O., Njoku, V.O. Adindu, C.B. and John-Dewole, O.O. Biosorption of Methylene Blue from Aqueous Solution using Unmodified Plantain Stalk (UPS) Biomass. Life Sci J 2024;21(10):8-14.
31. Katibi, K.K., Shitu, I.G., Yunos, K.F.M., Azis, R.S., Iwar, R.T., Adamu, S.B., Umar, A.M. and Adebayo, K.R., 2024. Unlocking the potential of magnetic biochar in wastewater purification: a review on the removal of bisphenol A from aqueous solution. *Environmental monitoring and assessment*, *196*(5), p.492.
32. Kundu, D., Sharma, P., Bhattacharya, S., Gupta, K., Sengupta, S. and Shang, J., 2024. Study of methylene blue dye removal using biochar derived from leaf and stem of Lantana camara L. *Carbon Research*, *3*(1), p.22.
33. Hellal, M.S., Attia, S.K., Kadimpati, K.K., Gnida, A. and Rashad, A.M., 2025. Preparation and characterization of an algal-based magnetic biochar nanocomposite for the removal of azocarmine G2 dye from aqueous solutions. *BMC chemistry*, *19*(1), p.123.
34. Mustapha, S.I., Muritala, K.B., Afolabi, A.M., Alhaji, M.H., Adewoye, T.L. and Aderibigbe, F.A., 2025. Phenol removal from pharmaceutical effluent using silver doped magnetite biochar: adsorption efficiency and kinetic studies. *Chemical Engineering Communications*, pp.1-21.
35. Zhang, S., Sun, X., Luo, Q., Chi, L., Sun, P. and Zhang, L., 2025. The Ce-modified biochar for efficient removal of methylene blue dye: Kinetics, isotherms and reusability studies. *Chinese Journal of Chemical Engineering*, *77*, pp.57-65.
36. Wang, L., Liang, L., Li, N., Chen, G., Guo, H. and Hou, L.A., 2025. A Mini-Review of Sludge-Derived Biochar (SDB) for Wastewater Treatment: Recent Advances in 2020–2025. *Applied Sciences*, *15*(11), p.6173.
37. Karce, H.E., Boumessaidia, S., Bahloul, A., Lal, B., Saravanan, A., Ouakouak, A., Hosseini-Bandegharaei, A., Sridevi, C. and Prakash, C., 2025. Efficient removal of methylene blue by a biochar from neem tree shell wastes using adsorption technology. *Biomass Conversion and Biorefinery*, *15*(9), pp.13559-13574.
38. Kiran, M., Haq, F., Mehmood, S. and Aziz, T., 2025. Innovative biosorbents from agro-waste: Advancing sustainable solutions for heavy metal, dye, and organic pollutant removal. *J Chem Eng Res Updates*, *12*, pp.1-33.
39. Zuhara, S., Pradhan, S., Zakaria, Y., Shetty, A.R. and McKay, G., 2023. Removal of methylene blue from water using magnetic GTL-derived biosolids: Study of adsorption isotherms and kinetic models. *Molecules*, *28*(3), p.1511.
40. Wang, D., Wang, X., Song, S., Hu, K., Wu, J. and Chen, Y., 2025. ZnCl2-modified almond shell-based biochar for highly efficient adsorption of crystal violet and methylene blue in water. *Biomass Conversion and Biorefinery*, pp.1-20.
41. Lomenech, C., Hurel, C., Messina, L., Schembri, M., Tosi, P., Orange, F., Georgi, F., Mija, A. and Kuzhir, P., 2021. A humins-derived magnetic biochar for water purification by adsorption and magnetic separation. *Waste and Biomass Valorization*, *12*(12), pp.6497-6512.

10/11/1015